



Highly sensitive silicon nanowire biosensor with novel liquid gate control for detection of specific single-stranded DNA molecules



Tijjani Adam*, U. Hashim

Institute of Nano Electronic Engineering (INEE), Universiti Malaysia Perlis (UniMAP), 01000 Kangar, Perlis, Malaysia

ARTICLE INFO

Article history:

Received 5 June 2014

Received in revised form

19 September 2014

Accepted 1 October 2014

Available online 6 October 2014

Keywords:

Nanowire biosensor

APTES

ssDNA

DNA

Photolithography

Liquid gate control

ABSTRACT

The study demonstrates the development of a liquid-based gate-control silicon nanowire biosensor for detection of specific single-stranded DNA (ssDNA) molecules. The sensor was fabricated using conventional photolithography coupled with an inductively coupled plasma dry etching process. Prior to the application of DNA to the device, its linear response to pH was confirmed by serial dilution from pH 2 to pH 14. Then, the sensor surface was silanized and directly aminated with (3-aminopropyl) triethoxysilane to create a molecular binding chemistry for biofunctionalization. The resulting Si–O–Si– components were functionalized with receptor ssDNA, which interacted with the targeted ssDNA to create a field across the silicon nanowire and increase the current. The sensor shows selectivity for the target ssDNA in a linear range from target ssDNA concentrations of 100 pM to 25 nM. With its excellent detection capabilities, this sensor platform is promising for detection of specific biomarkers and other targeted proteins.

© 2014 Elsevier B.V. All rights reserved.

1. Introduction

In complementary metal-oxide-semiconductors (CMOSs), the field-effect transistor (FET) response is determined by an oxide layer called the “gate.” Similarly, nanowire field effect transistor (NWFET) biosensors are generally equipped with a functional biointerface consisting of receptor molecules that serves the same purpose. This biointerface plays the key role in the detection of target biomolecules. The working principle is as follows: when a target molecule comes in close contact with the receptor, non-negligible partial charges appear in both the receptor and target molecules (Adam et al., 2013a, 2013c; Bashouti et al., 2013; Broomstrup et al., 2010). This modulates the surface charge profile of the functional layer (Chen et al., 2011, 2012), which affects the distribution of the electrostatic potential throughout the nanowire (Adam et al., 2013c; Lee et al., 2013). This in turn affects the conductance of the nanowire, and thus fluctuations in current can be detected when a voltage is applied at the appropriate terminals (De Vico et al., 2011; Kar, 2006; Chee et al., 2012). The amount of current response depends on the concentration of the target molecule in the liquid. This working principle is called liquid gate control.

In more detail, a FET conventionally has a source (S) terminal and a drain (D) terminal (De Vico et al., 2011; Mohammad et al., 2012). The solid gate discussed above controls the current passing between the source and drain (Nair and Ashraf Alam, 2007; Ramgir et al., 2010) by generating an electrical field. Semiconducting silicon nanowire biosensors work in much the same way (Adam et al., 2013a, 2013b, 2013c), but with a nanowire between the two conducting materials instead of a solid gate. A high concentration of atoms in a nanowire are located on its surface (i.e., it has a high surface-to-volume ratio), so the environmental conditions strongly affect the current as it passes from the source to the drain. In particular, the electrical properties the one-dimensional silicon nanowires are sensitive to their chemical surroundings. For example, if the number of adsorbed cations exceeds the number of adsorbed anions, the surface would gain an overall positive electric charge (Tricoli et al., 2010). This would cause the surface to be surrounded by a cloud of counter ions from the surface into the solution. The higher the partial charges on the material, the more ions will adsorb on the surface, and the larger the cloud of counter ions will be (Zhang et al., 2013). A solution with a higher concentration of electrolytes would also increase the size of the counter-ion cloud.

In the present work, we report a silicon nanowire biosensor with liquid gate control that is suitable for use in a liquid environment. To allow the device to interface with DNA capture probes, the sensing site was silanized and directly aminated with (3-aminopropyl) triethoxysilane (APTES) to create a so-called “molecular rug” binding chemistry. In particular, the Si–O–Si–

* Corresponding author. Fax: +60 4 9798578.

E-mail addresses: tijjaniamad@yahoo.com (T. Adam), uda@unimap.edu.my (U. Hashim).

components formed by silanization were bio-functionalized using APTES. The receptor single-stranded DNA (ssDNA) interacts with the targeted ssDNA to create a field across the silicon nanowire, which increases the measured current. With its excellent detection capabilities, this sensor platform is promising for detecting specific biomarkers and other targeted proteins.

2. Materials and methods

2.1. Materials

A 5-in. p-type (100) silicon-on-insulator (SOI) wafer and a two-contact chrome mask (wire and pad) were used for device fabrication. The chemicals used were (3-aminopropyl) triethoxysilane (APTES), glutaraldehyde, ethanolamine, and phosphate buffered saline (PBS, pH 7.4) and were obtained from Sigma-Aldrich (M) Sdn Bhd and used without further purification. The most important chemical used here was APTES. Its chemical formula is $C_9H_{23}NO_3Si$, and its molecular weight of 221.37 g/mol. APTES is clear liquid with density of 0.946 g/mL at 25 °C. It was tightly sealed and stored in a dry and well-ventilated place prior to use.

A Keithley semiconductor parametric analyser (SPA) was used for analysis, and buffered-oxide-etcher was used to remove organic and inorganic contaminants with the standard cleaning procedure using RCA1 and RCA2.

2.2. Fabrication of silicon nanowires

A 5-in. p-type silicon-on-insulator (SOI) wafer and a 250 nm insulator layer were coated with a 400-nm photoresist (PR) layer. After exposure and development, a pattern with a width between 3 μm and 5 μm was obtained; oxygen plasma etching was performed to reduce the size of the pattern to 200 nm, and a reactive ion etcher (RIE) was coupled with a high-temperature oxidation furnace to finally fabricate nanowires. Finally, the wire was trimmed by thermal oxidation with O_2 or H_2O . Afterward, Ti and Au were deposited on two ends of the patterned nanowire by a thermal evaporator. These steps are illustrated in Fig. 1.

The details of the five major photolithography processes listed above are as follows. First, the wafer is cleaned and coated with insulating material. In this study, we employed silicon oxide (SiO_2) as the insulator because it is inexpensive, widely used, and a good barrier layer for moisture and mobile ions (Wong, 2012). Then, silicon was deposited on by low-pressure CVD (LPCVD) using silane (SiH_4) to serve as the base material for the nanowires. Next, a thin layer (400 nm) of positive photoresist (+PR) was deposited, and the unwanted silicon on the wafer surface was etched to form silicon microwire with sizes of 1 μm using the chrome mask. After

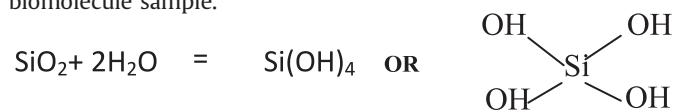
the microwires were formed, they were trimmed to the desired nanoscale sizes using plasma processes. In this step, oxide is grown on the surface of the microsized wire, which consumes the silicon, and is later etched away by the buffered oxide etcher. The amount of silicon consumed depends on the total penetration of the oxide, which is limited by the movement of the oxygen through the oxide–silicon interface.

2.3. Surface modification for gate control

Ion-supported attachment of specific capture probe oligonucleotides provides a powerful set of tools for identifying specific target DNA. In order to ensure that the targeted species are identified accurately, precisely, and reliably, the best method of attachment should be selected. An ssDNA probe can be covalently attached to a silicon nanowire using any of several methods. Carboxyl and amino groups are the most common reactive groups for attaching ligands to solid surfaces. Amino groups are very stable compared to carboxyl groups, and their chemistries have been widely explored by many research communities working in this field. Therefore, an amine-based approach is used in this study.

First, silicon oxide (SiO_2) deposited on the nanowire surface. While SiO_2 is one of the most important ingredients in FETs, it has excellent properties that makes it useful in every aspect of biosensing.

Then, water (H_2O) is passed over the deposited silicon oxide (SiO_2) in a furnace at 1000 °C to form $Si(OH)_4$. This makes the silicon nanowire surface hydroscopic by coating it with large amounts of $SiOH$, and it can thus readily adsorb ions from the biomolecule sample.



The ions migrate through the oxide materials and into the silicon nanowire itself, which causes electric changes in the material under a bias voltage. The ions are ultimately consumed when the strength of the electrical field increases, depending on the ion concentration. Through this process, the silicon-rich oxides can act as ion getters or barriers. Thus, an amine-terminated surface monolayer can be obtained by adding APTES to obtain surface-exposed $-NH_2$ (amine) groups. These can then be bioconjugated using a coupling reagent like glutaraldehyde to produce a surface that is reactive toward other amine groups. Therefore, after the formation of the $SiOH$ groups on the surface, the 3-APTES solution was coated to link glutaraldehyde to the surface. APTES is often used to prepare silane layers on silicon substrates for biomolecule immobilization with the help of glutaraldehyde linkers.

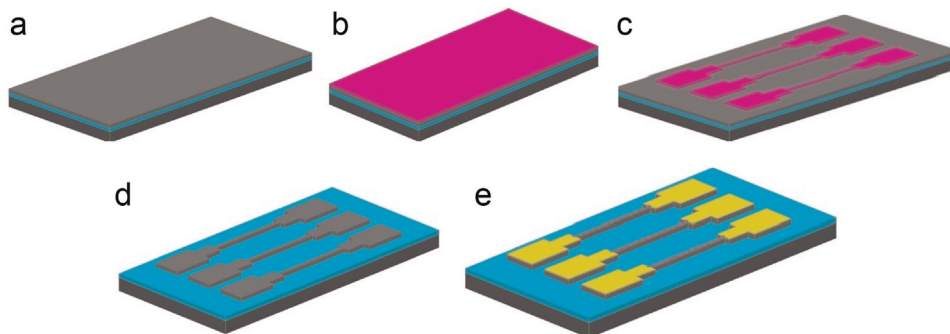


Fig. 1. Major steps of silicon nanowire-based FET device fabrication. (a) SOI wafer. (b) Resist coating. (c) Silicon pattern formation by lithography. (d) Resist development and washing. (e) Deposition of metal contacts for source and drain.

The next step was to attach the probe DNA. In this case, we use a hybridization probe, which is a single-stranded DNA sequence that can detect the presence of target nucleotide sequences that are complementary to the probe. Note, however, that both partial mismatches and full complements can be detected. The probe thereby hybridizes to single-stranded nucleic acid whose base sequence allows probe–target base pairing due to complementarity between the probe and target. The process is as follows: labeled DNA is first denatured (by heating or under-alkaline conditions such as exposure to sodium hydroxide) into single-stranded DNA (ssDNA-complementary) and then hybridized to the target ssDNA.

3. Results and discussion

3.1. Characterization of device trimming

The reaction between oxygen and silicon is diffusive in nature. In particular, at the atomic level, oxygen (and silicon) diffuses through the relatively open structure of the growing SiO_2 , as confirmed by Schaeffer (2012). To achieve anisotropic etching profiles with good aspect ratios for silicon nanowires, dry etching is preferred. This technique allows precise control of the etching depth and profiles because the incident ion energy, gas type, and pressure can be controlled more accurately than in traditional isotropic wet etching. However, in dry etching, there are very complicated interactions between these parameters, making the process development quite challenging when a smooth etch profile for smaller nanowires is needed.

In this study, we used two approaches to obtain the smallest possible nanowire dimensions without any damage to the substrate or the device. Inductively coupled plasma (ICP)-RIE was employed to trim the patterns from 1 μm in width down to 200 nm, and then wet etching was performed to reduce the wires from 200 nm down to approximately 10 nm. Fig. 2 shows FESEM image of the fabricated silicon nanowires after four successive trimming steps involving dipping into a 10:1 buffered oxide etcher (BOE) for 2 min of oxidation and subsequent ash trimming at 1000 °C until self-termination.

At the beginning of the oxidation process, oxygen atoms are inserted, leading to an expansion of the nanowire diameter by approximately 20%. At this point, no further ions penetrate into the silicon and no thus further oxidation occurs, because a huge compressive stress is concentrated in the oxide region near the SiO_2/Si interface. In fact, a Si core/ SiO_2 shell structure is formed, and the nanowire is never completely oxidized even if the trimming process is continued. This mechanism was also

supported by molecular dynamics simulations, which showed that ions will cease to penetrate into silicon as result of the compressive stress. Thus, this is a self-limiting oxidation technique that reduces the structures from around 1 μm in diameter to approximately 20 nm. The flux (number of molecules crossing a unit area per unit time) of oxidizing species from the bulk gas to the gas/oxide interface is different from the flux of the species from growing oxide to the silicon surface, and thus some of these oxidizing species react at the Si/SiO_2 interface, with yet another flux.

In order to monitor the device trimming process, the electrical conductance of the silicon nanowires was observed, and current–voltage (I – V) curves were obtained in the voltage range from 0 V to 10 V. However, the I – V curves obtained during ash trimming are not presented here. In summary, the combination of dry etching to 200 nm and subsequent wet etching yielded silicon nanowires with the desired dimensions. In particular, a well-defined shape is visible in Fig. 2.

Finally, the Au interconnect was photolithographically defined and Au was deposited after the last dry etching stage, followed by a lift-off process. Then, the sample was pre-treated with ultrathin titanium (Ti) to form an ohmic contact between the silicon nanowire and gold pads (Adam et al., 2013d,e). Once the trimming process was completed, the current–voltage (I – V) characteristics were measured by a Keithley 4200 Semiconductor Parameter Analyser. A typical I – V measurement setting was employed, where voltage was supplied to the source (S) region and output current was measured at the drain (D) region. For this experiment, devices with wire widths (W) of approximately 20 nm, 40 nm, 60 nm, and 80 nm were characterized. The details are not included here, but in general, the current decreased as the wire width became lower, indicating increases in resistance.

3.2. pH response

The pH-dependent current response was investigated using a standard two-probe I – V measurement set-up. A very low current is expected because of the high resistance of the silicon nanowires. For this purpose, a Keithley 2400 source meter with a current resolution of 10 pA was used. To determine the capability of the device, it was treated as a FET and subjected to various pH values. Since the surface of the device is hole-dominated (p-type material), it responds well to pH. In order to further strengthen this response, we protonated the surface of the silicon nanowire in a low-pH fluid to apply a positive surface charge. In particular, in a buffer solution of pH3, on the nanowire surface become positively charged $-\text{NH}_3^+$, which induces mobile carriers (holes) to form inside the nanowire. This approach was proposed by Lehoucq et al. (2012). Under these conditions, the nanowire surface acts as a positive top gate affecting the mobile carriers inside the nanowire (Barkelid and Steele, 2012). For example, when the surface of the silicon nanowire is deprotonated in lower pH liquid, the mobile carriers are depleted accordingly. When the modified p-type Si nanowire device was tested in solutions with pH 2 and 14, it exhibited stepwise increases in conductance. This is consistent with the results of a similar experiment performed by Swails et al. (2014), where the pH was changed stepwise from 2 to 14 manually using a dropper (Fig. 3).

In fact, the conductance increased approximately linearly with pH, which is excellent behavior from the standpoint of sensing. This behaviour results from the presence of two distinct receptor groups that are protonated/deprotonated over different pH ranges: silanol and ammonium groups. From a mechanistic standpoint, the increase in conductance with increasing pH is consistent with a decrease (increase) in the surface positive (negative) charge, which “turns on” the p-type FET through the accumulation of

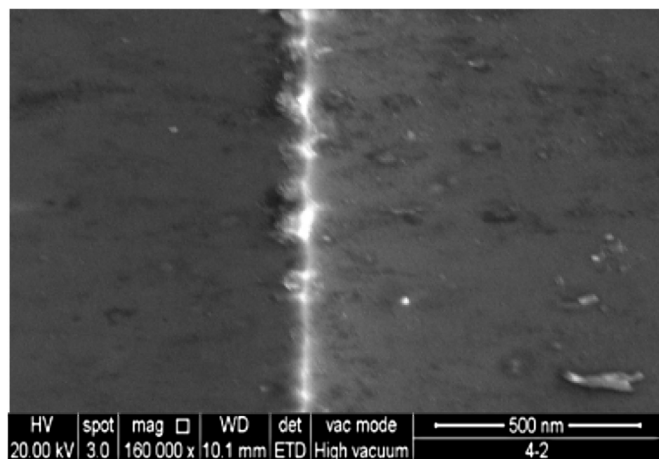


Fig. 2. Fabricated silicon nanowire device after trimming.

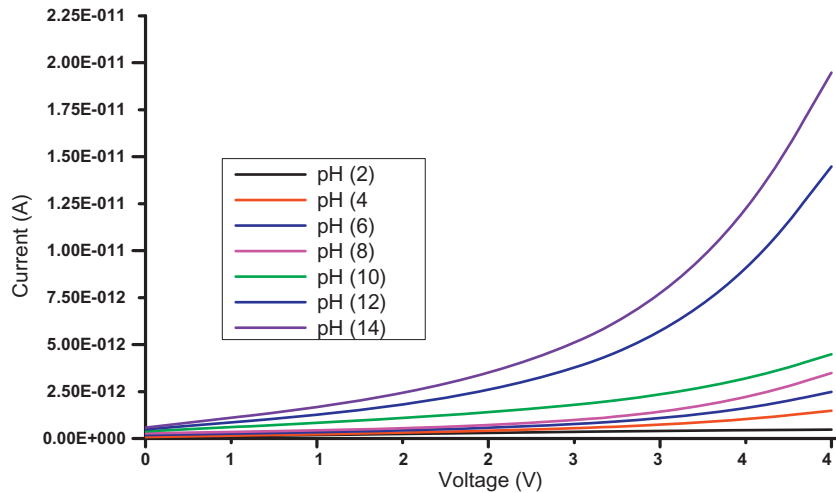


Fig. 3. Electrical response of silicon-nanowire-based detector to pH from 2 to 14.

carriers. The key role that the surface receptor plays in defining the response of the nanowire sensors was increasing the surface charge and reducing the resistance of the nanowire.

This mechanism was also demonstrated by [Lehoucq et al. \(2012\)](#). In particular, single charged molecules attached to the surface were examined, and the experienced by test charges at the silicon nanowires were simulated at different pH concentrations. The charge accumulation diminishes as the pH decreases and becomes negligible at pH 2 because more silanol surface groups are protonated, resulting in less negative charge on the silicon surface according to the reaction $\text{Si-OH} \rightleftharpoons \text{Si-O}^- + \text{H}^+$. The decrease in surface charge diminishes the charge accumulation as the acid concentration increases (pH decreases), which can be explained by DLVO theory ([Adamczyk and Weronski, 1999](#)). A high concentration of ions in the medium restricts the ion transfer and leads to more charge accumulation, since electrostatic interactions are stronger than the attractive van der Waals forces ([Adamczyk and Weronski, 1999](#)).

3.3. DNA detection by the silicon nanowire FET

Because silicon nanowires have a large surface-to-volume ratio, the device is sensitive to local charges in its environment ([Clément et al., 2011](#)). However, proper functionalization of its surfaces with

appropriate bimolecular or chemical receptors is needed for a selective response ([Clément et al., 2011](#); [Agrawal et al., 2009](#)). During the probe immobilization and DNA hybridization processes used for this purpose, the I - V characteristics were monitored to ensure the performance of the devices ([Fig. 4](#)). Upon immobilization of ssDNA, an increase in current of about 3 pA was recorded, and upon hybridization with a fully complementary DNA strand, a further significant increase in current was observed ([Duan et al., 2013](#)). The magnitude of this increase depended on the concentration of the complementary DNA strand, which is consistent with an increase in negative charge on the surface like that observed in the pH results above. The selectivity for a particular target molecule is typically achieved by attaching a specific recognition group to the surface of the Si-NW. In this study, a silicon oxide layer and uniform OH bonds were first added to the surface, as described above. Subsequently, the APTES solution was coated to link glutaraldehyde, and then the DNA oligomer could be bound effectively on the nanowire surface to react with the complementary DNA. The optimal grafting of APTES in this study was achieved by exploring the APTES concentration, silanization time, and silanization temperature.

As explained in [Section 2](#), a silicon oxide layer was formed on the exterior of the silicon nanowires as the first layer for the biomolecule attachment ([Kumar Gunda et al., 2014](#)). The -OH

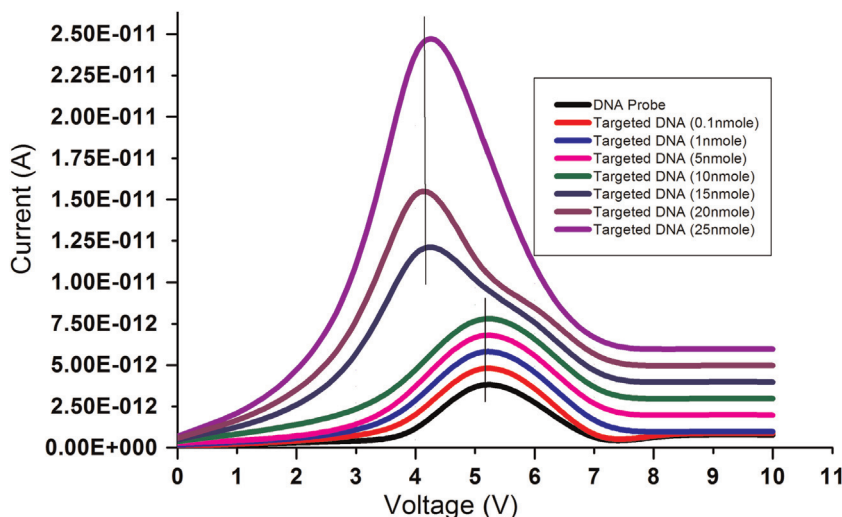


Fig. 4. I - V curves for silicon nanowire sensors. The surface is very sensitive to changes in the probe and targeted DNA concentrations, and conductivity increases consistently from 0.1 nM to 25 nM targeted DNA concentrations.

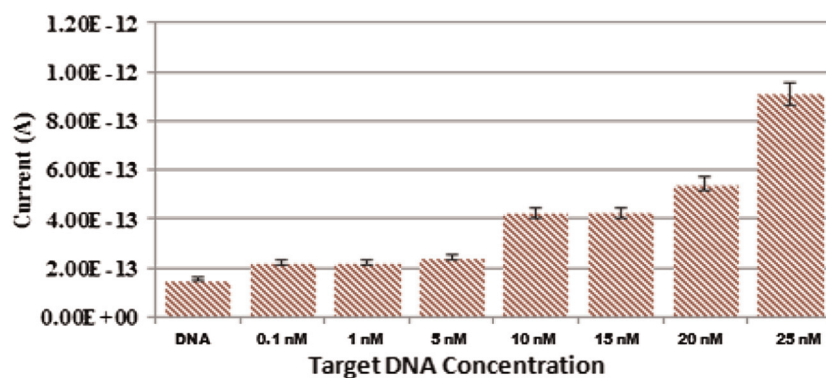


Fig. 5. Current measured with only probe DNA and with different concentrations of the targeted DNA. The error bars show the calculated standard deviations for repeated current measurements at each concentration.

groups were then hydrolysed to form siloxane bonds (Si–O–Si) with APTES, which can then immobilize the probe ssDNA (Sinko, 2010; Yang et al., 2012). The ability of APTES to bind to the probe ssDNA (5'-CTG ATA GTA GAT TTG TGA TGA CCG TAG AAA) was confirmed by observing the changes in surface charge of the nanowires after modification (Fig. 5). The increased negative charge results in an increase in current from 0 A to 3.0 pA. Kumar Gunda et al. (2014) made a similar observation in their study on the optimization of the silane layer thickness. Moreover, when the ssDNA target (5'CTA CGG TCA TCA CAA ATC TAC TAT CAG-3') was added to the solution, the current increased with increasing target ssDNA concentration. Thus, it can be concluded that the current increases with the concentration of targeted ssDNA mainly because the electrostatic interaction between the probe ssDNA and its complement affects the electrical properties and electron-transfer kinetics of the nanowire.

The sensitivity of the sensor was investigated in a series of solutions with different concentrations of the target ssDNA. The measured currents of the amine-based probe-DNA-modified silicon nanowire device for target ssDNA concentrations of 0.1, 1, 5, 10, 15, 20, and 25 nM are shown in Fig. 5. Clearly, the sensor could reliably detect the target DNA down to a 100 pM concentration. The reliability of the device for the detection of the target DNA in a linear range of concentrations from 100 pM to 25 nM was also examined, as indicated by the error bars. The current increases from about 0.5 pA for a 0.1 nM concentration to 1 pA for a 1 nM concentration. The mechanism of this response is as follows. As is well known, a negative gate voltage applied to a p-channel FET will create a conductive path from source to drain. This negative

charge causes the positive holes to move from the source and drain to the gate electrode and repels electrons from the n-type semiconductor body electrode further into the bulk structure. Therefore, the resistance in the space-charge region decreases, and current flow between the source and drain increases. A similar phenomenon occurs in the biomolecular sensor device. The hybridization between the targeted ssDNA and immobilised probe ssDNA on the silicon nanowire "gate" influences the gate potential. Thus, the target-recognition reaction directly influences the source–drain current. This causes the clear conductance changes shown in the figure. We thus conclude that the field-effect biosensing is based on changes in the charge distribution on the wire surface. In particular, the interaction between the ionic and phosphate groups of the DNA are electrostatic in nature and cause the formation of partial charges. When the targeted ssDNA molecule reacts with the immobilised probe ssDNA, the carrier density on the channel surface is modulated by the field effects of the electric charge of the biomolecules near the solid surface. Since DNA molecules possess negative charges, the density of surface holes increases with the concentration of these biomolecules.

The capability of the sensor for repeated detection of the targeted DNA was also investigated. Three different samples for each of the seven concentrations of targeted DNA were examined eight consecutive times at an interval of 24 h. The device was washed with salt water (50 mM NaCl) to dehybridize the DNA before subsequent hybridizations for this repeatability check for the same device. The hybridized double stranded oligonucleotides were washed again to immobilize the probe on the surface of the

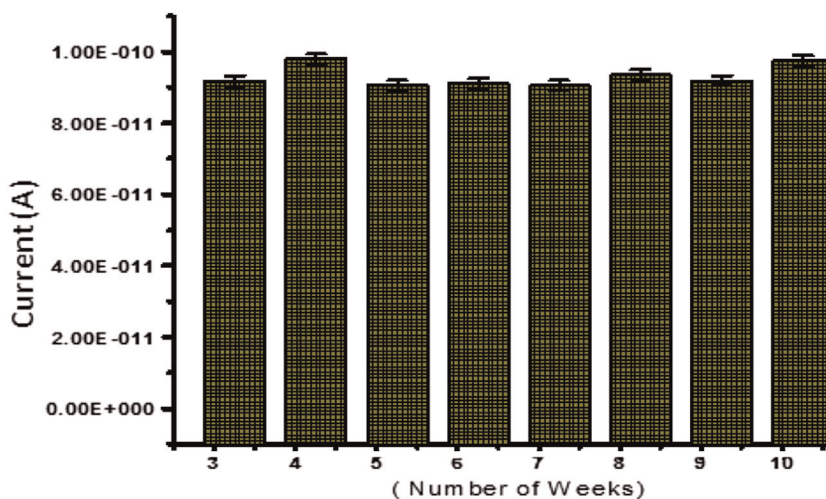


Fig. 6. Current response of the sensor to a 0.1 nM target ssDNA concentration measured over 10 weeks at an interval of 7 days.

sensor to obtain single-stranded surface-tethered sequences ready for further hybridization. These sequences were then hybridized again, and the results were compared with the previous results for the same device. The results show that the double-stranded conformation of DNA was completely detached from the sensor without causing any damage to the sensors. The sensor is capable of for 8 consecutive hybridization processes after washing, with an interval of 24 h (Fig. 6).

There is very little change among the repeated tests for any of the seven concentrations or for just probe DNA. In fact, 100% similarity was obtained for all consecutive tests, and the average values among the eight tests ranged from 96% to 100% with standard deviation values ranging from 1% to 5%. Thus, the sensor has high reusability and a minimum detection limit of well below 0.1 nM. However, further repeatability experiments could be needed for clinical applications. For example, testing intervals of more than one week should be investigated, and robust investigation of the reusability of this sensor over 1000 cycles of detection and regeneration is needed. The reliability tests were conducted using the same procedure described above. However, it is known that the response of the sensor is affected by factors such as the nanowire size and surface composition. Therefore, prior to the test, the response of the device was estimated based on the upper and lower concentrations used in this experiment. In particular, the current responses at 25 nM (G_{25}) and at 0.1 nM ($G_{0.1}$) were measured to define the following estimate of the device response:

$$\text{Device response} = \frac{G_{25} - G_{0.1}}{G_{25}} \times 100$$

The estimated device response is $\approx 95\%$, meaning that it can clearly detect concentrations as low as 0.1 nM because of the partial charges on the surface of the nanowire. For the purposes of the reliability test, only the smallest concentration (0.1 nM) was considered. The experiment clearly demonstrates the high sensitivity and reusability of the proposed sensor, which exhibits a response to specific molecular counter ions in a liquid environment.

4. Conclusion

We have demonstrated the development of a silicon nanowire liquid gate control sensor. The silicon nanowire is easily protonated and deprotonated in solutions with different pH, and thus can act as an ultra-sensitive pH sensor. Furthermore, biofunctionalized silicon could successfully detect specific DNA or protein molecules. The sensor selectively detects the target ssDNA, with a linear response to concentration from 100 pM to 25 nM. Thus, this sensor platform is promising for the detection of specific biomarkers and other targeted proteins and has the capability to work as a sensitive detector for sensing pH and charged molecules, down to the single-charge level. While semiconductor-based biosensors are fairly selective for the target molecule they are designed for, the degree of selectivity depends on the type of sensor, the target molecule, and its concentration. The best biosensor would have good selectivity for a single target molecule and be very reliable. The present study has demonstrated a device with a novel electric

response and potential for mass commercial fabrication that is highly selective and very reliable. Thus, we expect this system to be useful for point-of-care diagnostic applications.

Acknowledgement

The authors wish to thank the Universiti Malaysia Perlis UniMAP and Ministry of Higher Education Malaysia (Grant no. 9016-00004) for providing a COE-MTUN grant to conduct this research in the Micro & Nano Fabrication Lab. Much appreciation also goes to all the team members in the Institute of Nanoelectronic Engineering, especially the Nanostructure Lab-On-Chip Research Group.

References

- Adam, T., Hashim, U., Dhahi, Th.S., Foo, K.L., Leow, P.L., Son, P., 2013a. *Sens. Lett.* 11 (2), 333–336.
- Adam, T., Hashim, U., Dhahi, Th.S., Khor, K.N., Chee, P.S., Leow, P.L., Shahimin, M.M., Al Mufti, M.W., 2013b. *Wulfenia* 20 (1), 45–55.
- Adam, T., Hashim, U., Dhahi, Th.S., Leow, P.L., Chee, P.S., 2013c. *Curr. Nanosci.* 9, 543–551.
- Adam, T., Hashim, U., Foo, K.L., 2013d. *Adv. Sci. Lett.* 19 (1), 48–53.
- Adam, T., Hashim, U., Leow, P.L., Humayun, Q., 2013e. *Adv. Mater. Res.* 626, 1042–1047.
- Adamczyk, Z., Weroni, P., 1999. *Adv. Colloid Interface Sci.* 83, 137–226.
- Agrawal, R., Peng, B., Espinosa, H.D., 2009. *Nano Lett.* 9 (12), 4177–4183.
- Barkelid, M., Steele, G.A., Zwiller, V., 2012. *Nano Lett.* 12, 5649–5653.
- Bashouti, M.Y., Sardashti, K., Schmitt, S.W., Pietsch, M., Ristein, J., Haick, H., Christiansen, S.H., 2013. *Prog. Surf. Sci.* 88, 39–60.
- Bronstrup, G., Jahr, N., Leiterer, C., Csáki, A., Fritzsche, W., Christiansen, S., 2010. *ACS Nano* 4, 7113–7122.
- Chee, P.S., Arsat, R., Adam, T., Hashim, U., Rahim, R.A., Leow, P.L., 2012. *Sensors* 12 (9), 12572–12587.
- Chen, K.-I., Li, B.-R., Chen, Y.-T., 2011. *Nano Today* 6, 131–154.
- Chen, M.-C., Chen, H.-Y., Lin, C.-Y., Chien, C.-H., Hsieh, T.-F., Horng, J.-T., Qiu, J.-T., Huang, C.-C., Ho, C.-H., Yang, F.-L., 2012. *Sensors* 12, 3952–3963.
- Clément, N., Nishiguchi, K., Dufreche, J.F., Guerin, D., Fujiwara, A., Vuillaume, D., 2011. *Appl. Phys. Lett.* 98, 014104.
- De Vico, L., Iversen, L., Sorensen, M.H., Brandbyge, M., Nygard, J., Martinez, K.L., Jensen, J.H., 2011. *Nanoscale*, 3635–3640.
- Duan, X., Nitin, K., Rajan, D.A., Huskens, R.J., Reed, M.A., 2013. *ACS Nano* 7 (5), 4014–4021.
- Kar, S., 2006. *Appl. Surf. Sci.* 252 (11), 3961–3967.
- Kumar Gunda, N.S., Minashree, G.S., Normanc, L., Kamaljit, K., Mitra, S.K., 2014. *Appl. Surf. Sci.* 305, 522–530.
- Lee, S.H., Lee, T.I., Moon, K.J., Myoung, J.M., 2013. *ACS Appl. Mater. Interfaces* 5 (22), 11777–11782.
- Lehoucq, G., Bondavalli, P., Xavier, S., Legagneux, P., Abbyad, P., Baroud, C.N., Pribat, D., 2012. *Sens. Actuators*, 127–134.
- Mohammad, M., Hakim, A., Marta, L., Sun, K., Giustiniano, F., Roach, L., Davies, E.D., Howarth, P.H., Maurits, R.R., Planque, D., Morgan, H., Ashburn, P., 2012. *Nano Lett.* 12 (4), 1868–1872.
- Nair, P.R., M., Ashraf Alam, 2007. *IEEE Trans. Electron Devices* 54 (12), 3400–3408.
- Ramgir, N.S., Yang, Y., Zacharias, M., 2010. *Small* 6 (16), 1705–1722.
- Schaeffer, H.A., 2012. *J. Am. Ceram. Soc.* 64 (2), 156–161.
- Sinko, K., 2010. *Materials* 3, 704–740.
- Swails, J.M., York, D.M., Roitberg, A.E., 2014. *J. Chem. Theory Comput.* 10, 1341–1352.
- Tricoli, A., Righettoni, M., Teleki, A., 2010. *Angew. Chem. Int. Ed.* 49, 7632–7659.
- Wong, T.K.S., 2012. *Materials* 5, 1602–1625.
- Yang, X., Frenley, W.R., Zhou, D., Hu, W., 2012. *IEEE Trans. Nanotechnol.* 11 (3), 501–512.
- Zhang, L.G., Kaskhedikar, N., Cui, G., Maier, J., 2013. *ACS Appl. Mater. Interfaces* 5 (23), 12340–12345.